A novel small-scale self-focusing suppression method for the post-compression in high peak power lasers

Shuren Pan,[1,2,5] Fenxiang Wu,[1,5] Yang Zhao,[1] Jiabing Hu,[1] Zongxin Zhang,[1] Yi Xu,[1,4,6] Yuxin Leng,[1,4,7] Ruxin Li,[1] Efim Khazanov[3,4]

[1]*State Key Laboratory of High Field Laser Physics and CAS Center for Excellence in Ultra-intense Laser Science, Shanghai Institute of Optics and Fine Mechanics (SIOM), Chinese Academy of Sciences, Shanghai 201800, China*

[2]*Center of Materials Science and Optoelectronics Engineering, University of Chinese Academy of Sciences, Beijing 100049, China*

[3]*Gaponov-Grekhov Institute of Applied Physics (IAP) of Russian Academy of Science*

[4] *IAP-SIOM Joint Laser Laboratory*

[5]*These authors contribute equally to this work*

[6]*xuyi@siom.ac.cn*

[7]*lengyuxin@mail.siom.ac.cn*

Abstract: A novel method, combining an asymmetric four-grating compressor (AFGC) with the pulse post-compression, is numerically demonstrated to improve the spatial uniformity of laser beams and hence to suppress the small-scale self-focusing (SSSF) during the beam propagation in nonlinear materials of high peak power lasers. The spatial uniformity of laser beams is an important factor in performing post-compression, due to the spatial intensity modulation or the hot spots will be aggravated during the nonlinear propagation and then seriously damage the subsequent optical components. The three-dimensional numerical simulations of post-compression are implemented based on a femtosecond laser with a standard compressor and an AFGC, respectively. The simulated results indicate that the post-compression with AFGC can efficiently suppress the SSSF and meanwhile shorten the laser pulses from 30 fs to sub-10 fs. This work can provide a promising route to overcome the challenge of SSSF and will be meaningful to promote the practical application of post-compression technique in high peak power lasers.

1. Introduction

Thanks to the developments of chirped pulse amplification (CPA) and optical parametric chirped pulse amplification (OPCPA) [1-2] techniques, the laser peak power has reached 10 PW level, and the corresponding laser focused peak intensity has reached 10^{22} W/cm^2 and even 10^{23} W/cm^2 [3-6]. Such super-intense lasers can bring several significant breakthroughs and advance for high-field sciences [7-8]. Nowadays, some countries have also commissioned the construction of 100 PW level

This peer-reviewed article has been accepted for publication but not yet copyedited or typeset, and so may be subject to change during the production process. The article is considered published and may be cited using its DOI.

10.1017/hpl.2024.31

ultrahigh peak power lasers [9-12], to pursue higher laser intensity and hence to explore frontier sciences. As is well known, the laser peak power can be enhanced by increasing the pulse energy or by further shortening the pulse duration after the laser compressor. However, the limitation of peak power enhancement is no longer coming from the pulse amplification, but from the pulse compression which is restricted by the available size and damage threshold of compression gratings. A multifold enhancement of peak power can only be implemented by using mosaic gratings in laser compressors or coherent combination with several grating compressors. As a result, it entails a significant increase in the complexity, size, and cost of ultrahigh peak power lasers. Shortening the pulse duration after laser compressor, i.e., post-compression, is obviously a promising approach to further enhance the peak power of lasers which can be carried out without adding costly amplifiers and compression gratings. In addition, it is notable that the post-compression technique is also a potential way to develop compact and economical high peak power lasers.

The post-compression process generally consists of the spectral broadening and the pulse recompression [12-13]. For the post-compression of high peak power lasers, the spectral broadening based on solid thin plates has been proved to be one of the suitable ways to shorten pulse duration. As early as 2013, Aleksandr. A. Voronin et al. have proposed and simulated the generation of the subexawatt few-cycle pulse via the post-compression of a 13 PW / 120 fs laser [14]. In recent years, significant experimental progress has also been made in the post-compression of femtosecond lasers, with the peak power of hundreds-TW and even PW class [15-18].

Although the pulse post-compression technique features undisputed merits, there are still some problems hindering its implementation, especially the SSSF effect [19]. It can result in significant impairment of beam quality, uncontrollable spectral broadening, and the breakdown of optics. As is well known, the spatial intensity and phase modulation of high peak power laser are usually relatively high, which is mainly induced by the defects of high-energy pump lasers and large-size gain media. Besides, hot spots will also appear due to the diffraction on dusts or on optical defects. The spatial intensity modulation or the hot spots will be further aggravated during the nonlinear propagation process, then SSSF occurs and induces damage to optics. Hence, the SSSF suppression has become a key issue of the post-compression in high peak power lasers. On the one hand, SSSF can be suppressed by filtering the spatial perturbations during beam propagation in free space, i.e., beam self-filtering with a specific spatial distance [14-21]. On the other hand, the impacts of SSSF can be suppressed by improving the spatial uniformity of the laser beams before post-compression. To this end, the spatial filters were employed before laser compressor [14-15]. However, spatial filters are high-cost and complex. Especially for broadband high peak power lasers, spatial filters need to consider not only the vacuum environment, but also their aberrations and possibly chromatic effects.

In this work, the AFGC is numerically demonstrated for suppressing the SSSF during post-compression in high peak power lasers. The core of this method is to improve the spatial uniformity of laser before post-compression by using an AFGC. It can provide a promising route to overcome the challenge of SSSF in traditional post-compression. Recently, a work about the beam smoothing by introducing spatial dispersion was proposed for high peak power laser recompression [22]. But it focused on the inhomogeneity of spectral broadening and peak power enhancement induced by the spatial nonuniformity of laser beam, and the effect on SSSF suppression has not been investigated or proved. Differently, this work mainly focuses on the SSSF suppression by applying

https://doi.org/10.1017/hpl.2024.31 Published online by Cambridge University Press

an AFGC. To clearly reveal the SSSF and demonstrate the SSSF suppression by AFGC, three-dimensional simulations of post-compression with a higher-resolution are carried out based on a femtosecond laser with a standard compressor and an AFGC respectively. The numerical results show that the post-compression after AFGC can effectively suppress the SSSF and meanwhile shorten the pulses from 30 fs to sub-10 fs.

2. The post-compression after a standard compressor

The traditional post-compression for high peak power laser with a standard compressor (L_1=L_2) is shown as Fig. 1. The compressed laser beam is firstly spectral broadened through the nonlinear transmission in thin plates (TTPs), and then dispersion compensated by chirped mirrors (CMs).

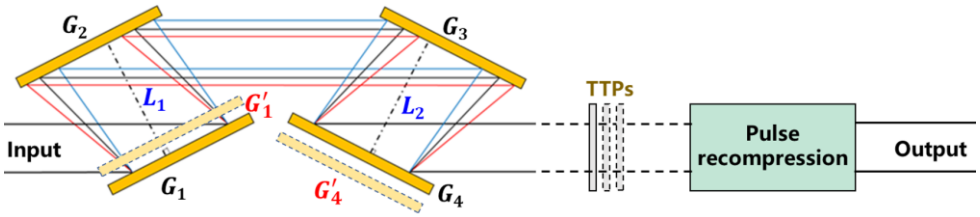

Fig. 1. Setup of post-compression in high peak power lasers with a standard compressor (G_1, G_2, G_3 and G_4, L_1=L_2) and an AFGC (G'_1, G_2, G_3 and G'_4, L_1≠L_2).

Assuming that the pulse spectrum (ranging from 750 nm to 850 nm) is 60 nm width at FWHM, the pulse duration is $\tau_{FWHM} = 30$ fs, the spatial beam fluence is a 10th super-Gaussian distribution, and the spatial noise is a sinusoidal distribution for simplicity. Its corresponding maximal peak intensity in numerical simulations is about 2.8 TW/cm^2. These parameters are set with reference to our SULF-1 PW laser beamline [3], which is a typical femtosecond high peak power laser. The nonlinear media for spectral broadening are fused silica TTPs, with the group delay dispersion (GDD) of ~36 fs^2/mm and the nonlinear refractive index of ~2.5×10^{-7} cm^2/GW at 800 nm central wavelength. The laser propagation in nonlinear media is simulated by a three-dimensional nonlinear Schrödinger equation [23], shown as Eq. 1. Here, A is the envelope of electric field strength, z is the longitudinal coordinate, t is the time, β_2 is the group velocity dispersion, ω_0 and k_0 are the central frequency and central wavenumber respectively, n_0 and n_2 are the linear and nonlinear refractive index respectively. As the gain spectra of modulation instability (also known as SSSF) [24] generally features a cutoff around hundreds of mm^{-1}, which corresponds to transverse uniformity of the beam profile with a typical size of a few microns, the resolution of our simulations is set as 2.5 μm. Besides, limited by the computing power, the beam diameter of only 9 mm is adopted for numerical simulations and verifications. But actually, the beam diameters of high peak power lasers are generally up to hundreds of millimeters.

$$\frac{\partial A}{\partial z} = \frac{i}{2k_0}\nabla_\perp^2 A + ik_0\frac{n_2}{n_0}|A|^2A - i\frac{\beta_2}{2}\frac{\partial^2 A}{\partial t^2} - k_0\frac{n_2}{n_0\omega_0}\frac{\partial(A\cdot|A|^2)}{\partial t}. \quad (1)$$

In the nonlinear propagation progress, an arbitrary transverse wavevector $K_\perp$ (K_0=2πn_0 / λ_0) propagates at an angle (θ=± $K_\perp$/ K_0) to the z axis. And the most serious characteristic angle is the direction in which the nonlinear process becomes phase matched, when considering the nonlinear contributions to the different characteristic angles. The most serious characteristic angle and corresponding spatial frequency can be calculated by Eq. 2 [12].

https://doi.org/10.1017/hpl.2024.31 Published online by Cambridge University Press

$$\theta_{max} = \sqrt{\frac{2n_2 I}{n_0}}; \qquad K_{\perp max} = K_0\theta_{max} = \frac{2\pi n_0}{\lambda_0}\sqrt{\frac{2n_2 I}{n_0}}. \tag{2}$$

For the 30 fs laser assumed above, the noise gain for different spatial frequency components is calculated, as shown in Fig. 2(a) [25-26]. The noise gain is calculated as the ratio of the noise fluences after and before spectral broadening process. For simplicity, the spatial frequencies of all noises in the laser are set to $K_{\perp max}$ (calculated result is ~350 mm^{-1}) in the following spectral broadening process. On the one hand, the SSSF instability has the highest increment at this spatial frequency. And hence, if suppression at the peak of the instability gain, which shows the maximal SSSF suppression ability of this method, is satisfied, we may not take much care about all other ones. On the other hand, the noises at this frequency cannot be completely diffracted out by the free propagation over a few meters in the compressors of ultrahigh peak power lasers, since the beam diameters of which generally reach up to hundreds of millimeters. And the beam cleaning in a standard compressor is not the point of this work, hence we neglected the temporal self-filtering in standard compressors [27].

To clearly show the physical nature of AFGC in SSSF suppression, we used 30 fs pulses at each point of the beam cross-section and fluence distribution as a boundary condition for Eq. 1 at z=0. The attainable recompressed pulse durations of the 30 fs laser are also calculated based on the different length of TTPs. As shown in Fig. 2(b), sub-10 fs recompressed pulses can be achieved in the case of 1.0 mm-thick fused silica TTPs, which has also been experimentally proved in a similar femtosecond laser [15]. Thereby, the 1.0 mm-thick fused silica plates will be employed for the spectral broadening in following simulations, with a B-integral of ~5.5.

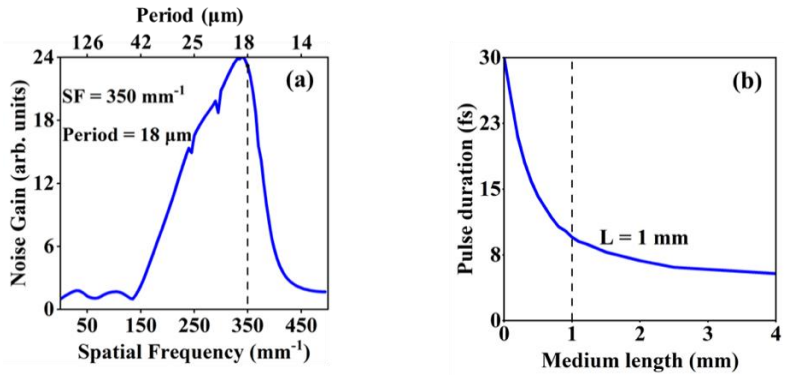

Fig. 2. (a) The noise gain for different spatial frequency components, (b) the relationship between the achievable recompression pulse durations and the length of fused silica TTPs.

Figure 3(a) illustrates the spatial distribution of initial 30 fs laser. The maximal beam fluence is 0.12 J/cm^2, the PTA (peak-to-average) of beam fluence is 1.52. The left and bottom curves correspond to the beam fluence on the central axis of laser beam, and the same to following figures. After passing through the 1.0 mm-thick fused silica TTPs, the fluence modulation get much more serious, and the maximal beam fluence greatly increases to 0.76 J/cm^2, shown as Fig. 3(b). Such a large beam fluence will seriously destroy the following optical components and prevent the practical application of post-compression. To reveal more detail, the small areas in Fig. 3(a-b) are zoomed in, shown as Fig. 3(c-d). It is obvious that serious SSSF occurs during above

https://doi.org/10.1017/hpl.2024.31 Published online by Cambridge University Press

spectral broadening progress. Hence, the suppression of SSSF should be a core issue in the post-compression of high peak power lasers.

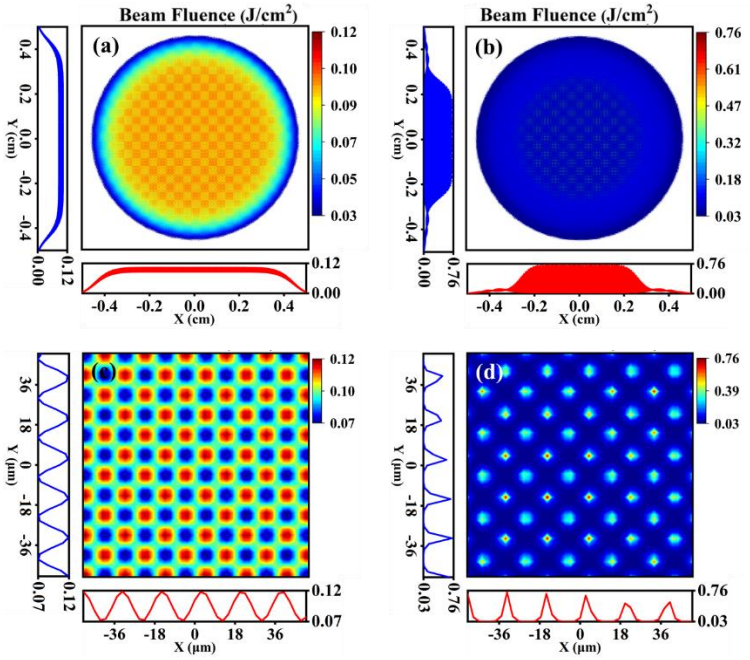

Fig. 3. The spatial beam fluences of 30 fs laser (a) output from a standard compressor and (b) then after spectral broadening. (c) and (d) are the larger versions of corresponding areas in (a) and (b) respectively.

3. The post-compression after an AFGC

The novel post-compression scheme based on AFGC [28], i.e., $L_1 \neq L_2$ in Fig. 1, is proposed for high peak power lasers, to overcome the challenge of SSSF. An AFGC can offer absolutely the same amount of temporal chirp for pulses compression like a standard compressor, as long as (L_2+L_1) are equal in both designs. Hence, the influence of residual temporal chirp on the following spectral broadening process can be ignored. By using the AFGC, a moderate spatial dispersion can be introduced to the output laser, which can effectively smoothen the beam fluence [28]. The AFGC induced spatial dispersion length can be written as Eq. 3. Where, ω_s and ω_l represents the shortest and the longest wavelength components of the input laser respectively, α and β are the incident and diffracted angles on G_1. It is obvious that the spatial dispersion length d_0 is proportional to the difference between L_1 and L_2. Since the relatively strong diffraction ability of gratings, large spatial dispersion can be realized just by a small (L_2–L_1).

$$d_0 = (tan\,\beta(\omega_s) - tan\,\beta(\omega_l)) \times cos\,\alpha \times (L_2 - L_1). \quad (3)$$

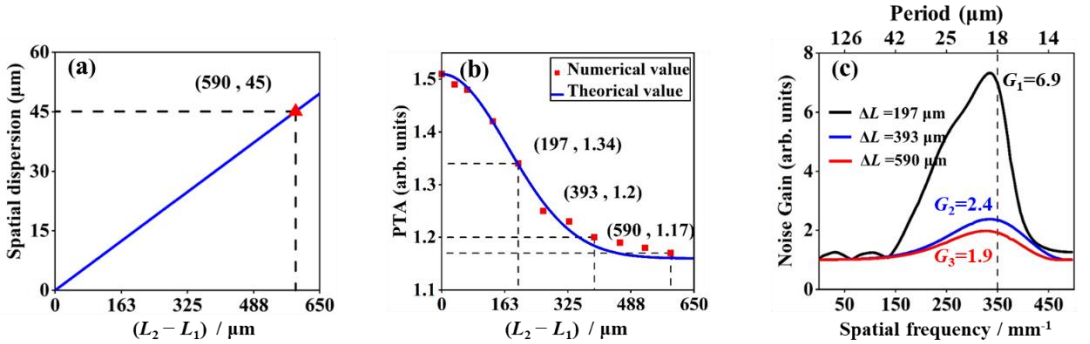

https://doi.org/10.1017/hpl.2024.31 Published online by Cambridge University Press

Fig. 4. The (a) spatial dispersion and the (b) the PTA of beam fluence output from AFGC, based on different (L_2–L_1) of AFGC. (c) The noise gain curves of laser beam after AFGC with different (L_2–L_1).

In order to demonstrate the advantages of AFGC in SSSF suppression, a numerical simulation is also carried out based on the same 30 fs laser parameters as above. For the standard compressor above, the grating groove density is 1480 gr/mm, the grating pair separations are 1.0 m, and the laser incident angle on G_1 is α =50°. These parameters are also referring to the compressor in our SULF-1 PW laser beamline [3]. To be an AFGC, two grating pair separations are altered respectively, while keeping their sum constant (2 m). Figure 4(a) shows that the spatial dispersion length d_0 is proportional to the difference between L_1 and L_2, and Figure 4(b) shows that the PTA drastically reduces with (L_2–L_1) increases. The numerical simulation agrees well with the theoretical prediction (blue curve), which is deduced using the Equations (8, 21, 27, 28, 32) in [27]:

$$PTA_{out} = exp\left(-\left(\frac{L_2 - L_1}{l}\right)^2\right)(PTA_{in} - PTA_{ideal}) + PTA_{ideal}. \quad (4)$$

where

$$l = \frac{\omega_0 \tau_{FWHM}}{\sqrt{ln2} \cdot k_{\perp max}} \cdot \frac{cos^3\beta(\omega_0)}{(sin\alpha + |sin\beta(\omega_0)|)cos\alpha}. \quad (5)$$

PTA_{ideal} =1.16 is the result of ideal 10th super-Gaussian beam without noise, and ω_0 represents the central wavelength component of input laser. The noise gain of the laser after AFGC is also reducing with the increase of (L_2–L_1), shown as Fig. 4(c). In the case of (L_1=0.999705 m, L_2=1.000295 m), the noise gain at 350 mm^{-1} is dramatically dropped to 1.9, while it is 24 when a standard compressor is adopted. This difference (L_2–L_1=590 μm) is very small compared with the initial grating pair separation of 1 m. Hence, the slight influence on the spatiotemporal quality of compressed pulses can be ignored [29]. Notably, the results in [27, 28, 30] have also proved that the temporal contrast and the focused peak intensity of compressed pulses output from an AFGC remains almost unchanged, compared with a standard compressor.

https://doi.org/10.1017/hpl.2024.31 Published online by Cambridge University Press

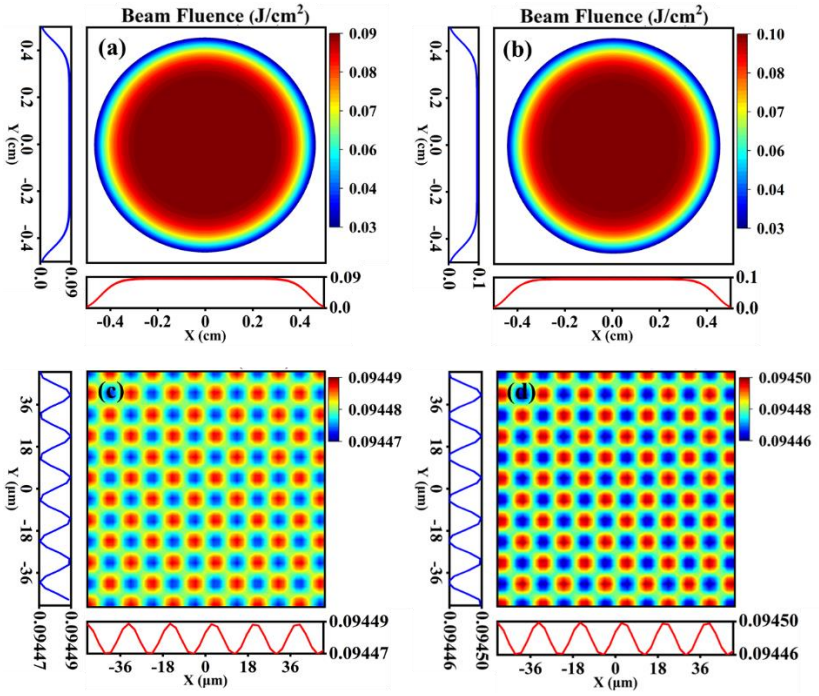

Fig. 5. The spatial beam fluence of 30 fs laser (a) output from an AFGC and (b) then after spectral broadening stage. (c) and (d) are the larger versions of corresponding areas in(a) and (b) respectively.

The beam fluence output from above AFGC is shown as Fig. 5(a). It is clear that the fluence modulation is greatly decreased, and the maximal beam fluence is reduced from initial 0.12 J/cm^2 to 0.09 J/cm^2. Then, the smooth laser beam will also pass through the 1.0 mm-thick fused silica TTPs for spectral broadening. The output beam fluence is shown as Fig. 5(b). As the noise gain is only 1.9, the maximal beam fluence is just increased to 0.09450 J/cm^2 from 0.09446 J/cm^2. And there is no evident degradation of the fluence modulation or the spatial uniformity in above spectral broadening process. The small areas which correspond to Fig. 3 are also zoomed in and shown as Fig. 5(c-d). Before and after the TTPs, there are no obvious difference for beam quality. This simulation results prove that the SSSF is effectively suppressed by the AFGC. Compared with Fig. 3(b), the SSSF induced fluence modulation and intensity spikes are overcome and a more uniform laser beam is achieved.

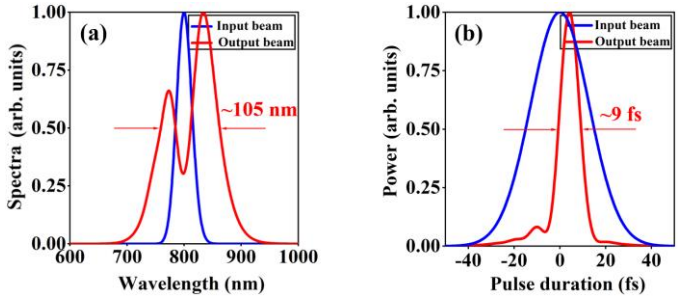

Fig. 6. (a) The spectra of laser pulses before and after spectral broadening, (b) the pulse durations before and after post-compression with an AFGC.

For the sake of simplicity, the spectral broadening and recompressing of above smooth laser beam are characterized by the simulated results based on nonlinear Schrödinger equation, in which the

https://doi.org/10.1017/hpl.2024.31 Published online by Cambridge University Press

laser intensity is approximated as the averaged intensity in the near-field. As a result, the spectral width is broadened from 60 nm to ~105 nm (FWHM), as shown in Fig. 6(a). The asymmetry of broadened spectrum is mainly induced by the self-steepening effect. Lastly, the residual dispersion of spectral broadened laser is compensated by using broadband CMs. The additional group delay dispersion (GDD), introduced by the SPM process and the nonlinear materials, is about 80 fs^2. After being reflected by two broadband CMs with a total GDD of -80 fs^2, sub-10 fs ultrashort laser pulses are expected, as shown in Fig. 6(b).

4. The post-compression with different initial noise intensity

For the initial laser beams with different noise intensity compared to Fig. 3(a), the PTA of the beam fluence after spectral broadening process and the corresponding noise gain are also investigated, as the upper two curves shown in Fig. 7(a) and 7(b). Due to the saturation effect, the PTA growth of output beam fluence gradually flatten out and the noise gain rapidly reduces, with the increase of initial noise fluence. Physically, the saturation can be explained by the reduction of fluence transferring from the main laser to the noise. When the noise fluence is high enough to be compatible with the main laser fluence, the instability increment decreases. In other words, the noise gain rapidly increases with the reduction of initial noise intensity, i.e., the PTA of initial beam fluence. And the noise gain can reach to ~2.4×10^4 when the initial PTA is 1.17. In this case, serious SSSF will occur in the post-compression with a standard compressor shown as Fig. 7(c) and 7(e), but a smooth laser beam still can be achieved by applying an AFGC (L_2-L_1=590 μm, the same in all cases) before the post-compression, shown as Fig. 7(d) and 7(f). Hence, AFGC may be also indispensable for the post-compression of high peak power lasers, even if the laser beams before nonlinear media are good enough.

https://doi.org/10.1017/hpl.2024.31 Published online by Cambridge University Press

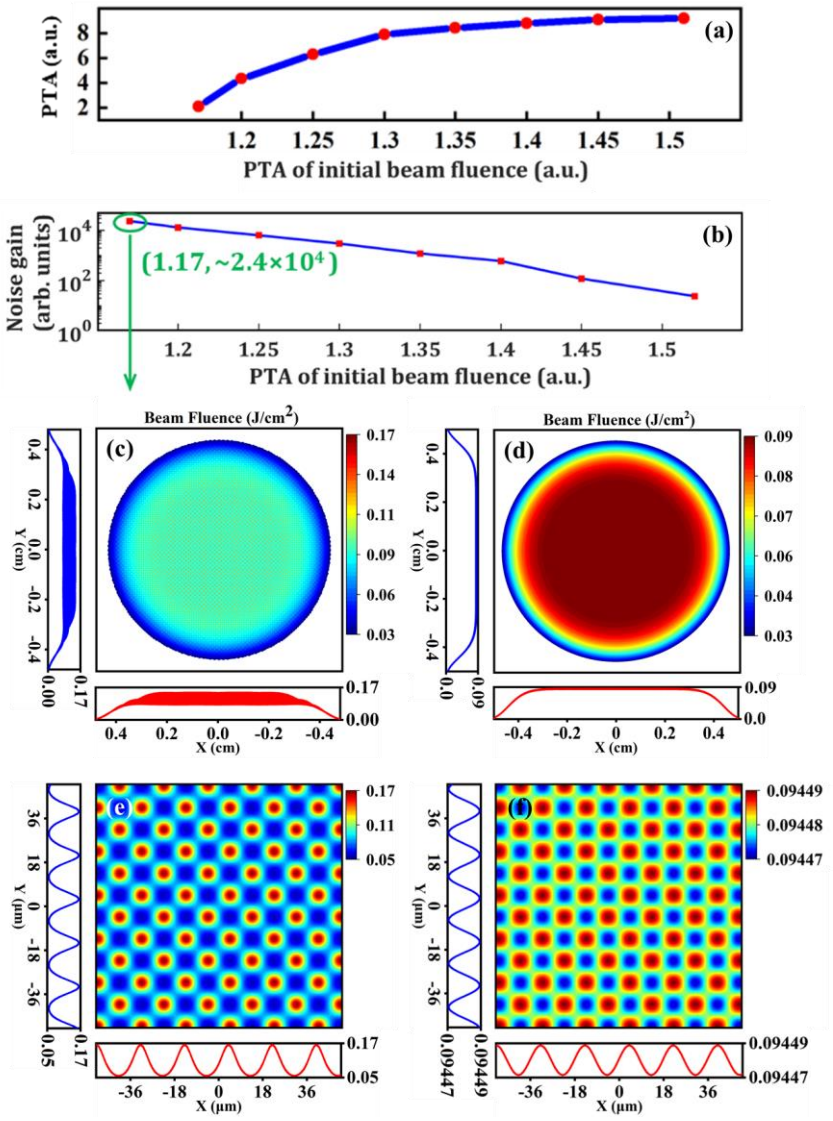

Fig. 7. (a) The PTA of the beam fluence after spectral broadening with 1 mm thick TTP and (b) the corresponding noise gain, based on different initial laser beams. The beam fluences of lasers after spectral broadening with 1 mm thick TTP, with (c) a standard compressor and (d) an AFGC, (e-f) are the larger versions of corresponding areas in (c-d) respectively.

5. Conclusion

In summary, a novel method is numerically proved to suppress the SSSF for the post-compression in high peak power lasers. The crucial point is the effective combination of an AFGC with post-compression, in which case the beam smoothing of AFGC can be fully utilized for the following post-compression. The numerical results indicate that AFGC can efficiently suppress the SSSF and meanwhile shorten the high peak power laser pulses from 30 fs to sub-10 fs. What's more, AFGC is also indispensable for the post-compression of high peak power lasers, even if the beam quality of lasers before nonlinear media are good enough. Hence, this method should be very meaningful to promote the practical application of post-compression in high peak power lasers.

Funding

National Key R&D Program of China (2022YFE0204800, 2022YFA1604401, 2019YFF01014401); Shanghai

https://doi.org/10.1017/hpl.2024.31 Published online by Cambridge University Press

Sailing Program (21YF1453800); The National Natural Science Foundation of China (11127901, 61925507); The International Partnership Program of Chinese Academy of Sciences (181231KYSB20200040); Shanghai Science and Technology Committee Program (22560780100, 23560750200); Chinese Academy of Sciences President's International Fellowship Initiative (2023VMB0008); Ministry of Science and Higher Education of the Russian Federation (075-15-2020-906, Center of Excellence "Center of Photonics"). The Youth Innovation Promotion Association of the Chinese Academy of Sciences.

Disclosures. The authors declare no conflicts of interest.

References

1. M. D. Strickland, G. Mourou, "Compression of amplified chirped optical pulses," Opt. Commun. **55**, 219 (1985).
2. Dubietis, G. Jonušauskas, A. Piskarskas, "Powerful femtosecond pulse generation by chirped and stretched pulse parametric amplification in BBO crystal," Opt. Commun. **88**, 437 (1992).
3. Z. Zhang, F. Wu, J. Hu, X. Yang, J. Gui, X. Liu, C. Wang, Y. Liu, X. Lu, Y. Xu, Y. Leng, R. Li, and Z. Xu, "The 1 PW / 0.1 Hz laser beamline in SULF facility," High Power Laser Sci. Eng. **8**, e4 (2020).
4. H. Kiriyama, Y. Miyasak, A. Kon, M. Nishiuchi, A. Sagisaka, H. Sasao, A. S. Pirozhkov, Y. Fukuda, K. Ogura, K. Kondo, N. P. Dover, M. Kando, "Enhancement of pre-pulse and picosecond pedestal contrast of the petawatt J-KAREN-P laser," High Power Laser Sci. Eng. **9**, e62 (2021).
5. J. W. Yoon, Y. G. Kim, I. W. Choi, J. H. Sung, H. W. Lee, S. K. Lee, C. H. Nam, "Realization of laser intensity over 10^{23}W/cm^2," Optica **8**(5), 630 (2021).
6. D. Umstadter, "Review of physics and applications of relativistic plasmas driven by ultra-intense lasers," Phys. Plasmas **8**, 1774 (2001).
7. W. Wang, K. Feng, L. Ke, C. Yu, Y. Xu, R. Qi, Y. Chen, Z. Qin, Z. Zhang, M. Fang, J. Liu, K. Jiang, H. Wang, C. Wang, X. Yang, F. Wu, Y. Leng, J. Liu, R. Li, Z. Xu, "Free-electron lasing at 27 nanometres based on a laser wakefield accelerator," Nature, **595**(7868), 516 (2020).
8. J. Bromage, S.-W. Bahk, M. Bedzyk, I. A. Begishev, S. Bucht, C. Dorrer, C. Feng, C. Jeon, C. Mileham, R. G. Roides, K. Shaughnessy, M. J. Shoup III, M. Spilatro, B. Webb, D. Weiner, J. D. Zuegel, "MTW-OPAL: a technology development platform for ultra-intense optical parametric chirped-pulse amplification systems," High Power Laser Sci. Eng. 9, e63 (2021).
9. E. Khazanov, A. Shaykin, I. Kostyukov, V. Ginzburg, I. Mukhin, I. Yakovlev, A. Soloviev, I. Kuznetsov, S. Mironov, A. Korzhimanov, D. Bulanov, I. Shaikin, A. Kochetkov, A. Kuzmin, M. Martyanov, V. Lozhkarev, M. Starodubtsev, A. Litvak, and A. Sergeev, "eXawatt Center for Extreme Light Studies," High Power Laser Sci. Eng. **11**, 78 (2023).
10. E. Cartlidge, "Eastern Europe's laser centers will debut without a star," Science **355**(6327), 785 (2017).
11. F. Wu, J. Hu, X. Liu, Z. Zhang, P. Bai, X. Wang, Y. Zhao, X. Yang, Y. Xu, C. Wang, Y. Leng, R. Li, "Dispersion management for a 100 PW level laser using a mismatched-grating compressor", High Power Laser Sci. Eng. **10**, e38, (2022).
12. E. A. Khazanov, S. Yu. Mironov, G. Mourou, "Nonlinear compression of high-power laser pulses: compression after compressor approach", Physics-Uspekhi **62**(11), 1096 (2019).
13. T. Nagy, P. Simon, L. Veisz, "High-energy few-cycle pulses: post-compression techniques", Adv. Phys. X **6**, 1 (2020).
14. A. A. Voronin, A. M. Zheltikov, T. Ditmire, B. Rus, and G. Korn, "Subexawatt few-cycle lightwave generation via multipetawatt pulse compression," Opt. Commun. 291, 299 (2013).
15. J. I. Kim, Y. G. Kim, J. M. Yang, J. W. Yoon, J. H. Sung, S. K. Lee, and C. H. Nam, "Sub-10 fs pulse generation by post-compression for peak-power enhancement of a 100-TW Ti:Sapphire laser," Opt. Express 30, 8734 (2022).
16. V. Ginzburg, I. Yakovlev, A. Zuev, A. Korobeynikova, A. Kochetkov, A. Kuzmin, S. Mironov, A. Shaykin, I. Shaikin, E. Khazanov, G. Mourou, "Fivefold compression of 250-TW laser pulses," Phys. Rev. A **101,** 013829 (2020).

https://doi.org/10.1017/hpl.2024.31 Published online by Cambridge University Press

17. V. Ginzburg, I. Yakovlev, A. Kochetkov, A. Kuzmin, S. Mironov, I. Shaikin, A. Shaykin, E. Khazanov, "11 fs, 1.5 PW laser with nonlinear pulse compression," Opt. Express **29**, 28297 (2021).
18. A. Shaykin, V. Ginzburg, I. Yakovlev, A. Kochetkov, A. Kuzmin, S. Mironov, I. Shaikin, S. Stukachev, V. Lozhkarev, A. Prokhorov, and E. Khazanov, "Use of KDP crystal as a Kerr nonlinear medium for compressing PW laser pulses down to 10 fs," High Power Laser Sci. Eng. **9**, e54 (2021).
19. S. Mironov, V. Lozhkarev, G. Luchinin, A. Shaykin, and E. Khazanov, "Suppression of small-scale self-focusing of high-intensity femtosecond radiation," Appl. Phys. B **113**, 147 (2013).
20. M. Martyanov, V. Ginzburg, A. Balakin, S. Skobelev, D. Silin, A. Kochetkov, I. Yakovlev, A. Kuzmin, S. Mironov, I. Shaikin, S. Stukachev, A. Shaykin, E. Khazanov, A. Litvak, "Suppressing small-scale self-focusing of high-power femtosecond pulses," High Power Laser Sci. Eng. **11**, e28 (2023).
21. V. N. Ginzburg, I. V. Yakovlev, A. S. Zuev, A. P. Korobeynikova, A. A. Kochetkov, A. A. Kuz'min, S. Yu. Mironov, A. A. Shaykin, I. A. Shaikin, E. A. Khazanov, "Compression after compressor: threefold shortening of 200-TW laser pulses," Quant. Electron. **49**(4), 29 (2019).
22. H. Xi, X. Tang, Y. Liu, J. Bin, Y. Leng, "Beam smoothing by introducing spatial dispersion for high-peak-power laser pulse compression" Opt. Express 31, 33754 (2023).
23. H. Zia, "Simulation of white light generation and near light bullets using a novel numerical technique," Communications in Nonlinear Science and Numerical Simulation **54**, 356 (2018).
24. V. I. Bespalov and V. I. Talanov, "Filamentary structure of light beams in nonlinear liquids," Pisma v JETF 2004, 79 (4), 178-182 3, 307-310 (1966).
25. E. S. Bliss, J. T. Hunt, P. A. Renard, G. E. Sommargwn, H. J. Weaver, "Effects of Nonlinear Propagation on Lases Focusing Properties" Quant. Electron. **12**(7), 402 (1976).
26. V. N. Ginzburg, A. A. Kochetkov, A. K. Potemkin, E. A. Khazanov, "Suppression of small-scale self-focusing of high-power laser beams due to their self-filtration during propagation in free space" Quant. Electron. **48**(4) 325 (2018).
27. E. Khazanov, "Reducing laser beam fluence and intensity fluctuations in symmetric and asymmetric compressors," High Power Laser Sci. Eng. **11**, 93 (2023).
28. X. Shen, S. Du, W. Liang, P. Wang, J. Liu, and R. Li, "Two-step pulse compressor based on asymmetric four-grating compressor for femtosecond petawatt lasers," Appl. Phys. B **128**, 159 (2022).
29. C. Wang, D. Wang, Y. Xu, and Y. Leng, "Full-aperture chirped-pulse grating compression with a non-uniform beam," Opt. Commun. **507**, 127613 (2022).
30. S. Du, X. Shen, W. Liang, P. Wang, J. Liu and R. Li, "A 100-PW compressor based on single-pass single-grating pair," High Power Laser Sci. Eng. 11 e4 (2023).

https://doi.org/10.1017/hpl.2024.31 Published online by Cambridge University Press